

Atomic Layer Deposition of Ferroelectric Bismuth Titanate $\text{Bi}_4\text{Ti}_3\text{O}_{12}$ Thin Films

Marko Vehkamäki,* Timo Hatanpää, Marianna Kemell, Mikko Ritala, and Markku Leskelä

Laboratory of Inorganic Chemistry, Department of Chemistry, University of Helsinki, P.O. Box 55, FI-00014 Helsinki, Finland

Received April 26, 2006. Revised Manuscript Received June 7, 2006

Bismuth titanate thin films were prepared by atomic layer deposition. Bismuth tris(bis(trimethylsilyl)-amide) $\text{Bi}(\text{N}(\text{SiMe}_3)_2)_3$ was used as the bismuth and titanium methoxide $\text{Ti}(\text{OMe})_4$ as the titanium precursor while water was used as the oxygen source. Self-limited growth of Bi–Ti–O films took place at a deposition temperature of 190 °C. The as-deposited Bi–Ti–O films showed surface morphologies atypical for amorphous ALD films, which may point either to partial bismuth reduction or to weak ordering of the deposited Bi–Ti–O during film growth. The Bi–Ti–O films postannealed at 750 °C crystallized to either pyrochlore $\text{Bi}_2\text{Ti}_2\text{O}_7$ -type structures, mixtures of the pyrochlore- and layered perovskite $\text{Bi}_4\text{Ti}_3\text{O}_{12}$ phases, or phase-pure $\text{Bi}_4\text{Ti}_3\text{O}_{12}$ depending on the Bi/(Bi + Ti) ratio in the film. Slightly Bi-rich films were found to result in the phase-pure $\text{Bi}_4\text{Ti}_3\text{O}_{12}$. After postannealing in O_2 at 600 °C 51 nm thick films deposited on Pt/SiO₂/Si substrates had a remanent polarization P_r and coercive field E_c of 0.5 $\mu\text{C}/\text{cm}^2$ and 24 kV/cm, respectively. The leakage current density was below 1 $\mu\text{A}/\text{cm}^2$ up to ± 1.6 V applied bias.

1. Introduction

Bismuth titanate $\text{Bi}_4\text{Ti}_3\text{O}_{12}$, which belongs to a family of layered perovskite compounds first observed by Aurivillius,¹ has been widely studied for use as a ferroelectric material in electronics and optics. $\text{Bi}_4\text{Ti}_3\text{O}_{12}$ single crystals have strongly anisotropic ferroelectric properties due to their layered perovskite structure. Although precise study of the structure indicates a monoclinic space group with $a = 5.450$ Å, $b = 5.4059$ Å, $c = 32.832$ Å, and $\beta = 90.01^\circ$,² in practice the structure is often regarded as orthorhombic as the β -angle is very close to 90°. The spontaneous polarization of $\text{Bi}_4\text{Ti}_3\text{O}_{12}$ single crystals is angled ca. 4.5° from the a – b plane, resulting in spontaneous polarizations P_s of 50 $\mu\text{C}/\text{cm}^2$ and 4 $\mu\text{C}/\text{cm}^2$, in the a – b plane and c -axis directions, respectively.³

In thin film ferroelectrics, especially in those having polycrystalline structures, remanent polarizations P_r lower than the maximum induced polarization P_s are typically observed. The anisotropy of the ferroelectric properties of the $\text{Bi}_4\text{Ti}_3\text{O}_{12}$ structure is also reflected in the properties of thin films, the remanent polarizations of which are strongly influenced by the film orientation. For example, Watanabe et al.⁴ observed that the P_r values of epitaxially grown c -axis-oriented MOCVD films increased from 0.2 to 1.5 $\mu\text{C}/\text{cm}^2$ when the film thickness was increased from 50 to 400 nm, while P_s equal to single-crystal values could be induced for

films with thicknesses of 150 nm and above. When also other than c -axis orientations are present, P_r values above 4 $\mu\text{C}/\text{cm}^2$ have been observed,^{5,6} and with films with randomly oriented grains much higher P_r and P_s values are achieved; for example, $P_r = 19.6$ $\mu\text{C}/\text{cm}^2$ and $P_s = 26.5$ $\mu\text{C}/\text{cm}^2$ were reported by Si and Desu⁷ for a randomly oriented 750 nm MOCVD film.

Controlled preparation of Bi–Ti–O films over large-area substrates is demanding due to the need to accurately control both film composition and thickness. Atomic layer deposition (ALD) is a deposition technique which has excellent large area uniformity and better film conformality than typically achieved with MOCVD.^{8,9} This is realized by using self-limiting surface reactions of one gas-phase reactant at a time, thus limiting the growth to a single chemisorption layer. Typically, a precursor such as a metal halide or metal alkoxide is supplied alternately with an oxygen source such as H_2O or O_3 , each precursor pulse followed by a purging of excess precursor from the reactor. ALD of binary oxides such as TiO_2 , ZrO_2 , HfO_2 , and Ta_2O_5 is straightforward, but deposition of multicomponent oxides such as $\text{Bi}_4\text{Ti}_3\text{O}_{12}$, SrTiO_3 , and $\text{SrBi}_2\text{Ta}_2\text{O}_9$ is more demanding due to the need to control the cation stoichiometry and the need of having compatible precursors and process conditions for multiple metals. Also, it is difficult to find suitable precursors for bismuth and alkaline earth metals. Precursors studied for ALD of bismuth-containing oxides include triphenyl bismuth,

* To whom correspondence should be addressed. E-mail: marko.vehkamaki@helsinki.fi.

(1) Aurivillius, B. *Ark. Kemi* **1949**, *1*, 463.

(2) Rae, A. D.; Thompson, J. G.; Withers, R. L.; Willis, A. C. *Acta Crystallogr.* **1990**, *B46*, 474.

(3) Cummings, S. E.; Cross, L. E. *J. Appl. Phys.* **1968**, *39*, 2268.

(4) Watanabe, T.; Saiki, A.; Saito, K.; Funakubo, H. *J. Appl. Phys.* **2001**, *89*, 3934.

(5) Gu, H.; Kuang, A.; Wang, S.; Bao, D.; Wang, L.; Liu, J.; Li, X. *Appl. Phys. Lett.* **1996**, *68*, 1209.

(6) Schuisky, M.; Härsta, A.; Khartsev, S.; Grishin, A. *J. Appl. Phys.* **2000**, *88*, 2819.

(7) Si, J.; Desu, S. B. *J. Appl. Phys.* **1993**, *73*, 7910.

(8) Ritala, M.; Leskelä, M. *Handbook of Thin Film Materials*; Nalwa, H. S., Ed.; Academic Press: New York, 2002; Vol. 1, pp 103–125.

(9) Suntola, T. *Thin Solid Films*, **1992**, *216*, 84.

$\text{Bi}(\text{Ph})_3$,^{10,11} and tris(1-methoxy-2-methyl-2-propanolato)-bismuth, $\text{Bi}(\text{mmp})_3$,^{12,13} but fully self-limiting growth of Bi–Ti–O films which would demonstrate ferroelectric properties has not been reported.

In a previous study we found that alternate reactions of bismuth tris(bis(trimethylsilyl)amide) $\text{Bi}(\text{N}(\text{SiMe}_3)_2)_3$ and H_2O can be used to mix bismuth into other oxides, such as Ta_2O_5 and SrTa_2O_6 .¹⁴ However, the growth of binary Bi_2O_3 was observed to be difficult compared to the mixed oxides. In this work Bi–Ti–O films were grown by mixing $\text{Bi}(\text{N}(\text{SiMe}_3)_2)_3$ – H_2O cycles with $\text{Ti}(\text{OMe})_4$ – H_2O cycles. The growth of binary oxide BiO_x is also examined; growth of binary TiO_2 from $\text{Ti}(\text{OMe})_4$ and H_2O was reported earlier by Pore et al.¹⁵ Film crystallization by postdeposition annealing is also studied. Electrical properties of the films are studied by preparing Pt/ $\text{Bi}_4\text{Ti}_3\text{O}_{12}$ /Pt/ SiO_2 /Si structures.

2. Experimental Section

Film Growth and Postdeposition Annealing. The Bi–Ti–O thin films were grown on silicon substrates in a flow-type F-120 reactor with a chamber pressure of roughly 10 mbar.⁹ N_2 (99.999%) prepared with a Labgas N2L nitrogen generator was used as the purging and carrier gas. $\text{Bi}(\text{N}(\text{SiMe}_3)_2)_3$ was synthesized with procedures described elsewhere.¹⁴ Titanium methoxide, $\text{Ti}(\text{OMe})_4$ (95%), was used as received from Aldrich. Precursors were evaporated inside the reactor at temperatures of 120 and 130 °C for $\text{Bi}(\text{N}(\text{SiMe}_3)_2)_3$ and $\text{Ti}(\text{OMe})_4$, respectively. Annealing treatments were done in a modified Carbolite tube furnace which could be evacuated and filled with O_2 or N_2 . A movable susceptor plate was used to rapidly insert the samples to the center of the furnace held at 500–750 °C.

Structural Characterization. A Bruker D8 Advance diffractometer/reflectometer was used both for measuring film thicknesses by X-ray reflectometry (XRR) and for the X-ray diffraction measurements. The film Bi/(Bi + Ti) cation fraction was measured with energy-dispersive X-ray spectrometry (EDS) and by using the GMRfilm program for the EDS data evaluation.¹⁶ A Hitachi S-4800 field-emission scanning electron microscope equipped with an Oxford Instruments INCA 350 EDS system was used for both FESEM imaging and gathering of the EDS data.

Capacitor Preparation and Electrical Measurements. Capacitors were prepared by first coating a thermally oxidized silicon wafer with ca. 40 nm Pt film and subsequently annealing the Pt film to improve adhesion to SiO_2 , then Bi–Ti–O films were grown with ALD, and finally circular Pt top electrode dots with an area of $5.2 \times 10^{-8} \text{ m}^2$ were evaporated. Different annealing treatments at 500–600 °C were used to crystallize the Bi–Ti–O layer. Capacitances and dielectric losses were measured with a HP 4284A LCR meter. A Keithley 2400 SourceMeter was used for measuring leakage currents. A modified Sawyer–Tower¹⁷ circuit was used for Q – V

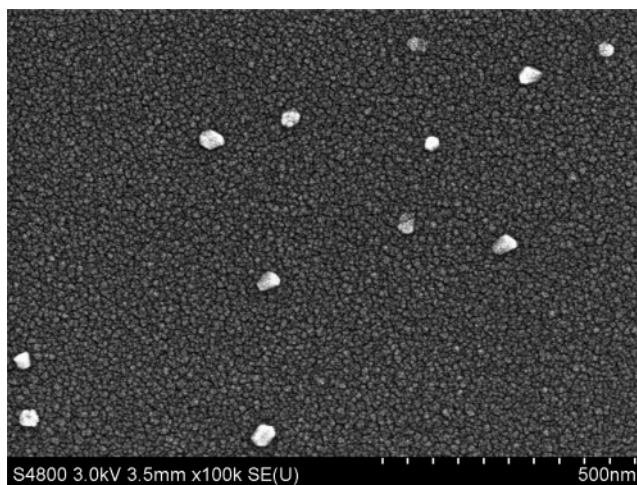


Figure 1. FESEM image of a BiO_x film grown on silicon with 2000 $\text{Bi}(\text{N}(\text{SiMe}_3)_2)_3$ – H_2O cycles.

measurements with an Agilent 33220A 20 MHz Arbitrary Waveform Generator serving as the 1 kHz sinusoidal signal source and with a National Instruments NI 5102 high-speed digitizer used for recording voltage signals.

3. Results and Discussion

Bismuth Oxide Deposition. First, it should be noted that the bismuth precursor $\text{Bi}(\text{N}(\text{SiMe}_3)_2)_3$ should be handled under inert gas atmosphere and preferably stored in dark as it is light-sensitive. $\text{Bi}(\text{N}(\text{SiMe}_3)_2)_3$ can be evaporated at 120–130 °C, but evaporation temperatures in excess of 130 °C should be avoided as they may lead to precursor decomposition in the solid state. Second, reaction temperatures above 200 °C should be avoided as rapid decomposition of $\text{Bi}(\text{N}(\text{SiMe}_3)_2)_3$ leading to formation of a silicon-containing deposit is observed around 225 °C. In our experiments the reaction temperature was set at 190 °C to give some safety margin against self-decomposition of the precursor.

In our previous study¹⁴ binary oxide BiO_x deposition was found difficult as large variation from one experiment to another was observed. A field-effect scanning electron microscope (FESEM) image of one BiO_x film grown on silicon with 2000 $\text{Bi}(\text{N}(\text{SiMe}_3)_2)_3$ – H_2O cycles is shown in Figure 1.

The flat small-granulated area seen in Figure 1 was 16 nm thick as measured by X-ray reflectivity (XRR) corresponding to a growth rate of 0.08 Å/cycle, which is somewhat low compared to the 0.1–0.2 Å/cycle growth rates observed in the earlier work. Larger grains with radius of about 30 nm are fairly uniformly distributed on the surface, with 100–300 nm grain-to-grain separation. Based on GIXRD measurement, the film is fully amorphous, so nucleation of crystallites does not explain the formation of such features. This is fairly intriguing as amorphous films deposited by ALD such as Al_2O_3 and Ta_2O_5 are usually completely featureless.

A possible explanation for the observed morphology and also the variation in the BiO_x growth is that part of the bismuth is reduced to metallic form during either the metal precursor pulse or the purging steps and then diffuses on the surface, coalescing to form small islands. For comparison,

(10) Schuisky, M.; Kukli, K.; Ritala, M.; Leskelä, M. *Chem. Vap. Deposition* **2000**, *6*, 139.

(11) Harjuoja, J.; Väyrynen, S.; Putkonen, M.; Niinistö, L.; Rauhala, E. *J. Cryst. Growth* **2006**, *285*, 376.

(12) Cho, Y. J.; Min, Y.-S.; Lee, J.-H.; Seo, B.-S.; Lee, J. K.; Park, Y. S. *Integr. Ferroelectr.* **2003**, *59*, 1483.

(13) Hwang, G. W.; Kim, W. D.; Min, Y.-S.; Cho, Y. J.; Hwang, C. S. *J. Electrochem. Soc.* **2006**, *153*, F20–F26.

(14) Vehkamäki, M.; Hatanpää, T.; Ritala, M.; Leskelä, M. *J. Mater. Chem.* **2004**, *14*, 1.

(15) Pore, V.; Rahtu, A.; Leskelä, M.; Ritala, M.; Sajavaara, T.; Keinonen, J. *Chem. Vap. Deposition* **2004**, *10*, 143.

(16) Waldo, R. A. *Microbeam Anal.* **1988**, 310.

(17) Sawyer, C.; Tower, C. *Phys. Rev.* **1930**, *35*, 269.

Schuisky et al. observed strong bismuth reduction when $\text{Bi}(\text{Ph})_3$ was studied as the bismuth source in ALD, resulting in metallic Bi in the films, observable by XRD.¹⁰ Surface diffusion of bismuth on different surfaces was studied by Terajima and Fujiwara, who observed average diffusion distances of 5–13 nm on mica surfaces at 175 °C during bismuth film deposition by evaporation in a high-vacuum system, and bismuth re-evaporation was considered to take place.¹⁸ Hwang et al. considered evaporation of bismuth during ALD as the cause of decrease in bismuth content in their films as they increased the deposition temperature from 225 to 300 °C in their $\text{Bi}_2\text{Ti}_2\text{O}_7$ process.¹³ In our process the deposition temperature and pressure are 190 °C and 5–10 mbar, respectively, with N_2 carrier gas as the main species in the gas phase. The nonvolatility of bismuth metal in our reactor conditions was verified by placing metallic Bi films separately prepared by electron beam evaporation into the reactor. No mass transport or change of morphology was seen to take place in a metallic Bi film for 10 h at 190 °C, even when the surface was subjected to $\text{H}-\text{N}(\text{SiMe}_3)_2$ vapor pulses supplied from an external reservoir. The protonated ligand $\text{H}-\text{N}(\text{SiMe}_3)_2$ is likely formed in the surface reactions and was thus suspected as a possible reducing agent. Pulsing $\text{H}-\text{N}(\text{SiMe}_3)_2$ on a BiO_x film or Bi_2O_3 , also tested in the reactor, did not cause reduction or any change in morphology, so formation of the features seen in BiO_x most likely takes place during the $\text{Bi}(\text{NSiMe}_3)_2$ pulse. The features observed in BiO_x are more likely due to surface migration than gas-phase migration.

As metallic bismuth melts at 271.3 °C, an annealing treatment of the BiO_x film shown in Figure 1 was done at 300 °C in a N_2 atmosphere for 1 h in order to see if significant morphological changes take place. No change was observed in FESEM images or GIXRD pattern of annealed BiO_x , so if bismuth reduction indeed takes place on the surface of the growing film, it seems likely that reoxidation has followed during further deposition cycles.

Bismuth Titanate Deposition. Mixing the BiO_x growth cycles with TiO_2 , Ta_2O_5 , or SrTa_2O_6 growth cycles makes the growth reproducible, probably by stabilizing the surface of the growing film. Adding $\text{Ti}(\text{OMe})_4-\text{H}_2\text{O}$ cycles in a 1:1 ratio gives films with a $\text{Bi}/(\text{Bi} + \text{Ti})$ cation fraction of 0.25 by EDS. The films have a much more homogeneous structure compared to BiO_x , as seen in Figure 2 a. When the Bi:Ti cycle ratio is increased (Figures 2b–2g), the surface morphology varies depending on the resulting $\text{Bi}/(\text{Bi} + \text{Ti})$ cation fraction in the film. All Bi–Ti–O films are amorphous as-deposited. Some kind of reduction/reoxidation is assumed to be the cause of the surface features of the Bi–Ti–O films similar to BiO_x , but now the growth is reproducible; different growth experiments with for example 7:1 Bi:Ti cycle ratio produce very closely the same thickness, composition, and surface morphology. The number and size of surface features increases in mixed Bi–Ti–O films compared to those in BiO_x .

Figure 3 shows the average growth rate and the $\text{Bi}/(\text{Bi} + \text{Ti})$ cation fraction as measured by EDS acquired with

different Bi:Ti cycle ratios. It is seen that the growth rate of a mixed Bi–Ti–O is equal to or larger than that of binary TiO_2 deposited at this temperature. The growth rate of Bi–Ti–O films, calculated by dividing the film thickness by the total number of binary oxide cycles, is above 0.2 Å/cycle when the Bi:Ti cycle ratio is between 1:1 and 1:3, but with more than four subsequent $\text{Bi}(\text{N}(\text{SiMe}_3)_2)_3-\text{H}_2\text{O}$ cycles the average growth rate drops below 0.2 Å/cycle. It will be seen that a sufficient Bi content for obtaining phase-pure $\text{Bi}_4\text{Ti}_3\text{O}_{12}$ by postdeposition annealing is reached with a 7:1 Bi:Ti cycle ratio, or 87.5% $\text{Bi}(\text{N}(\text{SiMe}_3)_2)_3-\text{H}_2\text{O}$ cycle fraction. Saturation of the film growth rate and $\text{Bi}/(\text{Bi} + \text{Ti})$ cation fraction as measured by EDS as a function of the $\text{Bi}(\text{N}(\text{SiMe}_3)_2)_3$ pulse length with a 7:1 Bi:Ti pulse ratio is shown in Figure 4. Self-limiting growth is taking place with a saturated growth rate of 0.18 Å/cycle, and the $\text{Bi}/(\text{Bi} + \text{Ti})$ cation fraction as measured by EDS varies between 0.58 and 0.61 with pulse lengths of 1 s and above.

Postdeposition Annealing and Structural and Electrical Characterization. Crystallization of the films by postdeposition annealing in O_2 was studied in the temperature range 500–750 °C. The measured $\text{Bi}/(\text{Bi} + \text{Ti})$ composition was not observed to change during postdeposition annealing steps. All annealing treatments were done by quickly moving the samples on a susceptor plate to a preheated segment of a tube furnace. First, postdeposition annealing in O_2 at 750 °C for 10 min was done for as-deposited Bi–Ti–O films taken from the growth experiments made with 3:1 to 7:1 cycle ratios, which were shown in Figures 2c–2g and 3. Bismuth oxide and titanium oxide form a group of ternary oxides, of which only the $\text{Bi}_2\text{Ti}_2\text{O}_7$ -type pyrochlore structure and the layered perovskite $\text{Bi}_4\text{Ti}_3\text{O}_{12}$ were observed in this study. Stoichiometric $\text{Bi}_2\text{Ti}_2\text{O}_7$ has only recently been characterized in single crystal form due to the fact that it is not an equilibrium phase and readily decomposes to $\text{Bi}_4\text{Ti}_3\text{O}_{12}$ and other more stable bismuth titanates. This was demonstrated for example in the work of Radosavljevic et al. who successfully prepared single crystals with a stoichiometry of $\text{Bi}_{1.74}\text{Ti}_{2.00}\text{O}_{6.62}$,¹⁹ but this required adding an excess of TiO_2 as mixtures with 1:1 Bi:Ti ratio formed a $\text{Bi}_4\text{Ti}_3\text{O}_{12}$ secondary phase. Phase-pure stoichiometric $\text{Bi}_2\text{Ti}_2\text{O}_7$ was eventually prepared by Hector and Wiggin who were able to isolate crystals by annealing them at a low temperature of 470 °C, above which a $\text{Bi}_4\text{Ti}_3\text{O}_{12}$ impurity began to form.²⁰

The preference for the $\text{Bi}_4\text{Ti}_3\text{O}_{12}$ formation is observed in the ALD Bi–Ti–O films as well, as seen in Figure 5. Only the pyrochlore phase was observed in annealed films grown with a 3:1 Bi:Ti cycle ratio and having a $\text{Bi}/(\text{Bi} + \text{Ti})$ of 0.44 by EDS, nominally $\text{Bi}_{1.56}\text{Ti}_{2.00}\text{O}_{6.34}$. The pyrochlore phase was also observed by Schuisky et al. in postdeposition annealed Bi–Ti–O films grown by ALD from $\text{Bi}(\text{Ph})_3$.¹⁰ With Bi:Ti cycle ratios from 4:1 to 6:1 and corresponding $\text{Bi}/(\text{Bi} + \text{Ti})$ by EDS in the range of 0.49–0.56, mixtures of pyrochlore and $\text{Bi}_4\text{Ti}_3\text{O}_{12}$ were observed, with only a small amount of pyrochlore present with a 6:1 Bi:Ti cycle ratio (Figure 5). Films with a $\text{Bi}/(\text{Bi} + \text{Ti})$ cation fraction of 0.58

(18) Terajima, H.; Fujiwara, S. *Thin Solid Films* **1975**, *30*, 55.

(19) Radosavljevic, I.; Evans, J. S. O.; Sleight, A. W. *J. Solid State Chem.* **1998**, *136*, 63.

(20) Hector, A. L.; Wiggin, S. B. *J. Solid State Chem.* **2004**, *177*, 139.

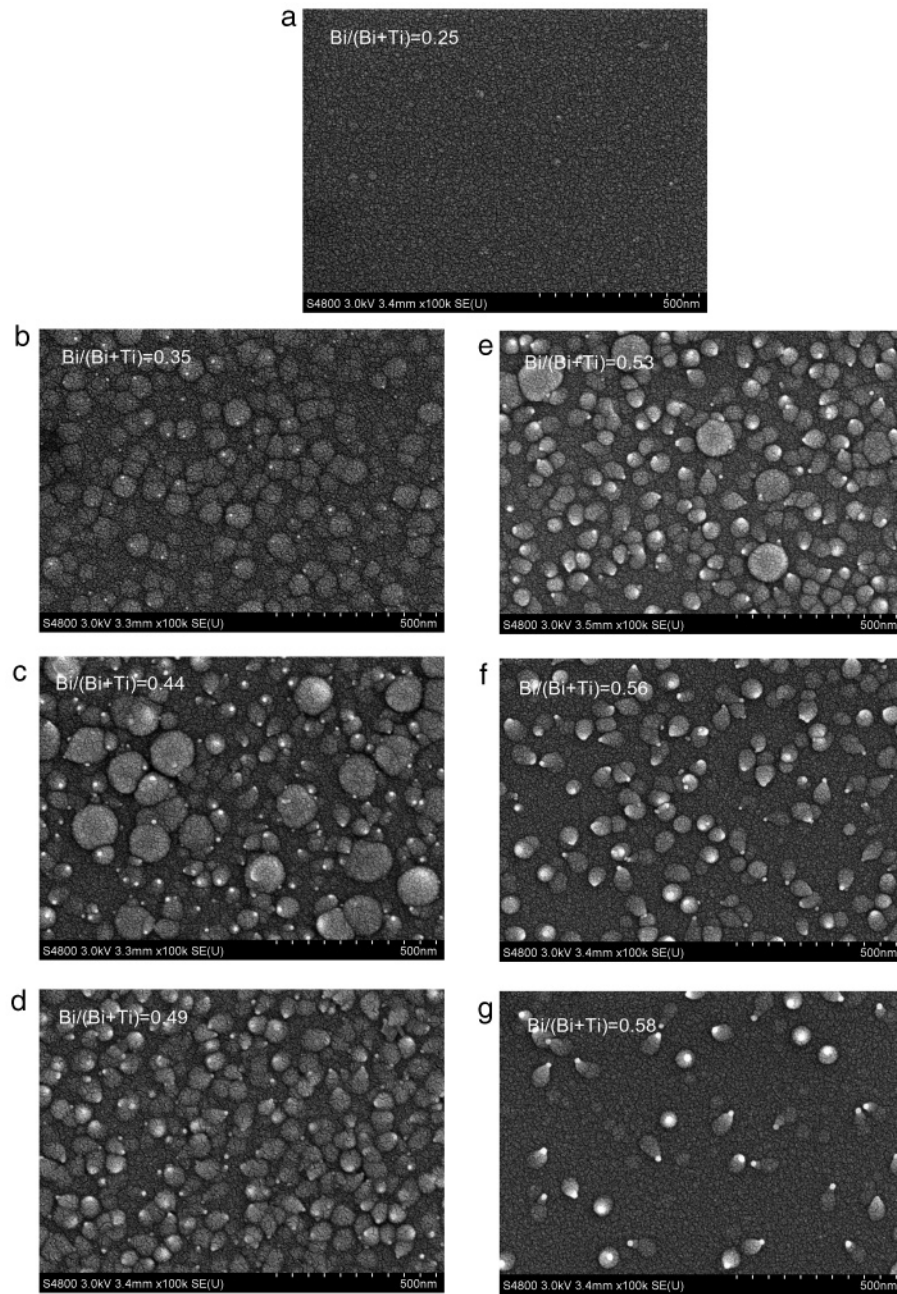


Figure 2. FESEM images of as-deposited Bi–Ti–O films grown with a total number of 3000 deposition cycles with different Bi:Ti cycle ratio. The Bi:Ti cycle ratios and the resulting film thicknesses were (a) 1:1 and 73 nm, (b) 2:1 and 86 nm, (c) 3:1 and 69 nm, (d) 4:1 and 65 nm, (e) 5:1 and 57 nm, (f) 6:1 and 56 nm, and (g) 7:1 and 51 nm. Displayed in the upper left corner of the figures are the Bi/(Bi + Ti) cation fractions as measured by EDS.

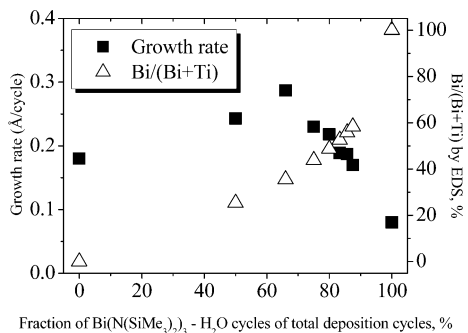


Figure 3. Bi/(Bi + Ti) cation fraction by EDS and growth rate as a function of the Bi(N(SiMe₃)₂)₃–H₂O cycle fraction of the total deposition cycles.

by EDS grown with 7:1 Bi:Ti cycle ratio, corresponding to a Bi excess of roughly 2%, were phase-pure Bi₄Ti₃O₁₂. It is

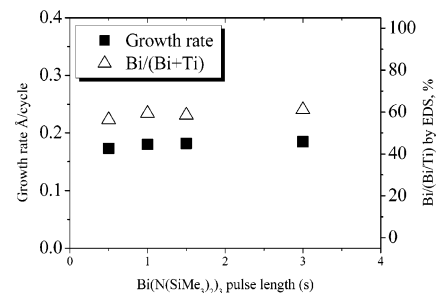


Figure 4. Saturation of the film growth rate and bismuth cation fraction Bi/(Bi + Ti) by EDS as a function of the Bi(N(SiMe₃)₂)₃ pulse length with a fixed 7:1 Bi:Ti cycle ratio.

notable that when excess bismuth is present, the Bi₄Ti₃O₁₂ crystallizes in a *c*-axis orientation, most likely due to an interaction with the silicon substrate.

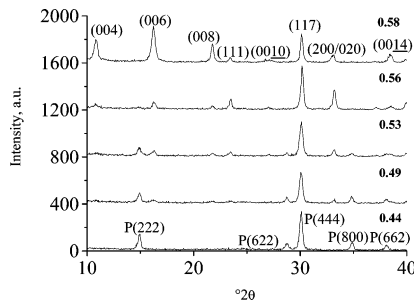


Figure 5. GIXRD patterns of Bi-Ti-O films annealed in O_2 at 750 °C for 10 min, with Bi/(Bi + Ti) as measured by EDS of (a) 0.44, (b) 0.49, (c) 0.53, (d) 0.56, and (e) 0.58. The notation $P(hkl)$ is used for the pyrochlore phase; the (hkl) indices denote the layered perovskite phase.

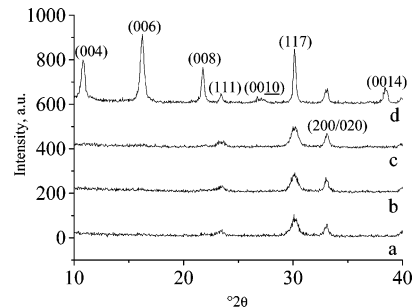


Figure 6. GIXRD patterns of a 51 nm Bi-Ti-O film with Bi/(Bi + Ti) = 0.58 by EDS grown on Si and annealed in O_2 at (a) 600 °C for 10 min, (b) 600 °C for 30 min, (c) 650 °C for 10 min, and (d) 10 min at 750 °C.

The crystallization of films with slight Bi excess was also studied as a function of the annealing temperature. Weak initial crystallization to the layered perovskite phase was observed already at 500 °C, with improved crystallinity observed for films annealed at 600–650 °C (Figure 6). The orientation of the films crystallized at 500–650 °C was random. This is fairly similar to the crystallization behavior observed for metal-organic decomposition (MOD) fabricated films with 15 mol % excess bismuth.²¹

Bi-Ti-O films were deposited on Pt/SiO₂/Si substrates with a total of 3000 reaction cycles and a 7:1 Bi:Ti cycle ratio in order to study the ferroelectric properties of the annealed layers. Thickness of the films was 51 nm. Prior to evaporation of top electrode dots, the films were annealed at 300 °C in O_2 for 10 min. After Pt top electrode evaporation the capacitor stacks were annealed first at 500 °C in order to cause initial random nucleation of $\text{Bi}_4\text{Ti}_3\text{O}_{12}$. Without this preannealing, films grown on platinum films and annealed directly at 600 °C in O_2 became *c*-axis oriented and had high loss, high leakage, and no measurable remanent polarization. The permittivities of these films at 0 V bias were above 100. When capacitors preannealed at 500 °C were annealed at 600 °C for 1 h, stable ferroelectric behavior could be observed. Figure 7 shows a FESEM image of the top surface of $\text{Bi}_4\text{Ti}_3\text{O}_{12}$ annealed for 10 min at 500 °C and 60 min at 600 °C. The initial morphology of the amorphous film does not seem to clearly influence the structure of the annealed film. The dielectric properties were observed to be sensitive to the annealing time and temperature, with too short 1–10 min annealing times at 600 °C resulting in high loss samples, possibly due to a high concentration of oxygen vacancies.

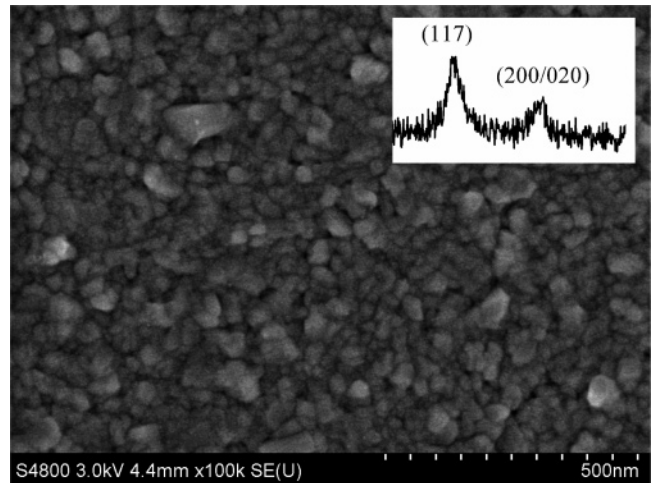


Figure 7. FESEM image of $\text{Bi}_4\text{Ti}_3\text{O}_{12}$ crystallized on Pt/SiO₂/Si surface next to a Pt top electrode dot. GIXRD pattern of the film in the image is seen in the inset, indicating the $\text{Bi}_4\text{Ti}_3\text{O}_{12}$ phase.

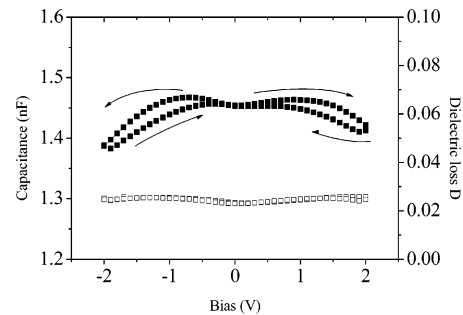


Figure 8. Capacitance and loss factor of a Pt/51 nm $\text{Bi}_4\text{Ti}_3\text{O}_{12}$ /Pt capacitor as a function of the bias voltage.

Capacitors annealed at 600 °C for 30–60 min had reasonably low loss of 0.02–0.03 at ± 2 V bias. The first few C - V sweeps of a capacitor annealed for 1 h at 600 °C did not show a stable C - V loop, but after subjecting the devices to a sinusoidal poling signal with 1 kHz frequency and 4 V peak-to-peak amplitude for 1 min, stable C - V and Q - V hysteresis was observed.

The capacitance and dielectric loss as a function of the bias voltage in the range of ± 2 V is shown in Figure 8 for a capacitor annealed at 600 °C for 1 h. The observed butterfly loop is due to switching of the ferroelectric polarization. The flatness of the C - V loop close to 0 V can be due electrode interface effects. Electrode interface effects such as trap states can become increasingly significant in very thin ferroelectric films. The permittivity calculated from the 0 V capacitance was 160, and the dielectric loss remained below 0.03. Increasing the bias further to ± 2.5 V showed a sharp increase in the dielectric loss, but dielectric breakdown did not take place for most samples. A 3 V bias caused a propagating breakdown in all tested devices.

Figure 9 shows the dc leakage current densities measured for both polarities. Separate sweeps were used for the opposite polarities. A 5 s measurement delay time was used after each 0.1 V step. It can be seen that higher overall leakage is measured with bottom electrode positively biased, i.e., when electrons are injected from the top electrode. This may be due to the top interface roughness of the Bi-Ti-O layer. The current densities remain below $1 \mu\text{A}/\text{cm}^2$ in the ± 1.6 V bias range, but at -2 V bias the current injected

(21) Du, X.; Chen, I.-W. *J. Am. Ceram. Soc.* **1998**, *81*, 3253.

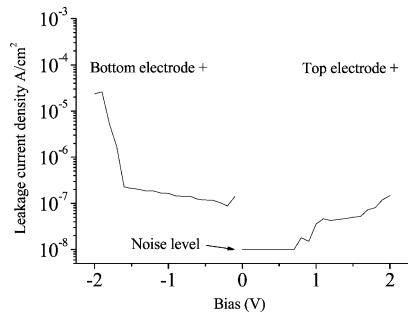


Figure 9. dc leakage current densities of a Pt/51 nm $\text{Bi}_4\text{Ti}_3\text{O}_{12}$ /Pt capacitor. A separate voltage sweep was used for positive and negative polarities, with positive polarity measured first. The applied voltage was ramped in 0.1 V steps with a 5 s delay before measurement of the current.

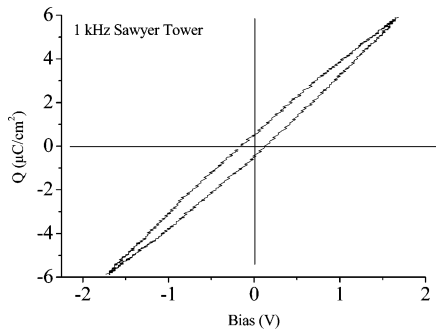


Figure 10. Q - V loop of a Pt/51 nm $\text{Bi}_4\text{Ti}_3\text{O}_{12}$ /Pt capacitor measured with a 1 kHz sinusoidal signal.

from the top interface is 2 orders of magnitude higher than that with the opposite bias.

Sawyer-Tower Q - V measurements (Figure 10) were done with a 1 kHz sinusoidal signal, with ± 1.7 V peak voltages applied across the device. A symmetric remanent polarization $\pm P_r$ of $0.5 \mu\text{C}/\text{cm}^2$ ($2P_r = 1 \mu\text{C}/\text{cm}^2$) was observed. The coercive voltage and field were 0.12 V and 24 kV/cm, respectively. When signal amplitudes higher than ± 2 V were used, apparently higher polarizations up to $\pm P_r = 1 \mu\text{C}/\text{cm}^2$ were observed in the Q - V loops. These higher polarizations can be due to injected charge rather than actual ferroelectric polarization, however, because high losses were

seen in the C - V sweeps with higher than 2 V bias. The data presented in Figures 8–10 are from the same single device, and the I - V data in Figure 9 were measured after the Q - V measurement shown in Figure 10, verifying reasonable resistivity in the Q - V sweep voltage range. Although $\pm P_r = 0.5 \mu\text{C}/\text{cm}^2$ is small compared to most values reported in the literature, it should be noted that usually reported results for $\text{Bi}_4\text{Ti}_3\text{O}_{12}$ capacitors have involved devices with much thicker > 200 nm layers, demonstrating ALD as a promising alternative for deposition of thin layers with ferroelectric compositions. In the future partial substitution of bismuth with other metals could be useful in order to prepare improved ferroelectric²² and dielectric²³ compositions.

4. Conclusions

Bismuth titanate films were prepared by ALD in a self-limiting manner by mixing $\text{Bi}(\text{N}(\text{SiMe}_3)_2)_3$ - H_2O and titanium methoxide- H_2O cycles. The films had morphologies atypical of amorphous ALD deposited films, with small protrusions in the 10–30 nm range observable in the FESEM images. At this point the most likely reason for this effect was assumed to be a partial reduction of bismuth, indicating that less reducing source chemicals could prove useful. The final morphology was dominated by the postdeposition annealing treatments, however, and test capacitors could be fabricated by carefully tuning the postdeposition treatments. The films could be crystallized to the ferroelectric $\text{Bi}_4\text{Ti}_3\text{O}_{12}$ phase. A remanent polarization of $0.5 \mu\text{C}/\text{cm}^2$ was measured for a 51 nm film, with a coercive voltage and coercive field of 0.12 V and 24 kV/cm, respectively.

Acknowledgment. We thank ASM Microchemistry Ltd. and Finnish National Technology Agency TEKES for financial support.

CM060966V

- (22) Park, B. H.; Kang, B. S.; Bu S. D.; Noh T. W.; Lee, J.; Jo, W. *Nature* **1999**, *401*, 682.
 (23) Takahashi, K.; Suzuki, M.; Oikawa, T.; Kojima, T.; Watanabe, T.; Funakubo, H. *Chem. Vap. Deposition* **2006**, *12*, 136.